Publication Year	2019
Acceptance in OA	2020-12-10T13:03:29Z
Title	Characterization of ammonium dihydrogen phosphate crystals for soft X-ray optics of the Beam Expander Testing X-ray facility (BEaTriX)
Authors	FERRARI, CLAUDIO, BERETTA, SARA, SALMASO, Bianca, PARESCHI, Giovanni, TAGLIAFERRI, Gianpiero, BASSO, Stefano, SPIGA, Daniele, Pelliciari, Carlo, GIRO, Enrico
Publisher's version (DOI)	10.1107/S1600576719004631
Handle	http://hdl.handle.net/20.500.12386/28777
Journal	JOURNAL OF APPLIED CRYSTALLOGRAPHY
Volume	52

Characterization of ADP crystals for soft X-ray optics of the Beam Expander Testing X-ray facility (BEaTriX)

Authors

Claudio Ferrari[a]*, Sara Beretta[a], Bianca Salmaso[b], Giovanni Pareschi[b], Gianpiero Tagliaferri[b], Stefano Basso[b], Daniele Spiga[b], Carlo Pelliciari[c] and Enrico Giro[b]

[a] IMEM-CNR Insitute, parco Area delle Scienze 37/A, Parma, PR, 43124, Italy

[b] INAF - Osservatorio Astronomico di Brera, via E. Bianchi 46, Merate, LC, 23807, Italy

[c]MPE, Max Plank Insitute for Extraterrestrial Physics, Gautinger Str.45, Neuried, 82061, Germany

Correspondence email: claudio.ferrari@imem.cnr.it

Synopsis A crystal of Ammonium Dihydrogen Phosphate (ADP) is characterized from the point of view of crystallographic quality and presence of residual strain. The crystal quality is fundamental in view of its use in a new X-ray facility BEaTriX for testing Silicon Pore Optics modules of the ATHENA X-ray telescope.

Abstract A new type of X-ray facility, the Beam Expander Testing X-ray facility (BEaTriX), has been designed and is now under construction at INAF-Osservatorio Astronomico di Brera to perform the acceptance tests of the Silicon Pore Optics modules of the ATHENA x-ray telescope. Crystals of elevate perfection and large dimensions are needed in order to obtain a wide beam (20x6 cm^2) with an x-ray divergence < 0.5 arcseconds and a x-ray energy purity $\Delta E/E<10^{-5}$. To generate x-ray diffracted beams at a x-rays energy of 1.49 keV, ADP crystals have been considered among other possible choices, because of their reported crystal quality and because they can be grown at sufficiently large size at reasonable price. In the present paper, the results of the characterization of crystalline quality and lattice planarity of a 20x20x2 mm^3 ADP sample are reported.

Keywords: X-ray astronomy; ADP crystal crystalline perfection; X-ray topography of ADP; Residual strain and lattice plane curvature measurement

1. Introduction

ATHENA (Advanced Telescope for High Energy Astrophysics) is an ESA X-ray mission aimed at understanding the evolution of the universe and the key role of the black holes. The 2.4 m diameter optics is composed by more than 700 Mirror Modules (MM) that need to be tested and accepted

IMPORTANT: this document contains embedded data - to preserve data integrity, please ensure where possible that the IUCr Word tools (available from http://journals.iucr.org/services/docxtemplate/) are installed when editing this document.

before integration. To this end, INAF-Osservatorio Astronomico di Brera started in 2012 to design a facility based on the generation of a broad, uniform and low divergent X-ray beam to illuminate the full aperture of the ATHENA MM with a beam with vertical and horizontal divergence lower than 1.5 arcseconds Half Energy Width (HEW) (Spiga *et al.*, 2012; Spiga *et al.*, 2014; Pelliciari *et al.*, 2015; Spiga *et al.*, 2016). The facility is now under construction for the 4.51 keV energy, and it is built to host the second beam line at 1.49 keV. The two energies are required to accept the MM, by measuring their Point Spread Function (PSF) and Effective Area.

For each line, the design foresees a X-ray microfocus source, a paraboloidal mirror, a symmetrical channel cut crystal as monochromator, and an asymmetrically-cut crystal for beam expansion. The vertical divergence of the final beam is limited by the 30 μm dimension of the focal spot of the X-ray source, whereas the horizontal divergence is also defined by the X-ray monochromators and by the asymmetrically cut crystal for the beam expansion (Salmaso *et al.*, 2018). Four reflections on a monochromation system made by symmetrically cut crystals are needed to reduce the bandwidth of the beam and limit the horizontal divergence, which is highly dependent on the energy dispersive properties of the asymmetrically cut crystal (del Rio *et al.*, 1992).

For the fulfillment of the projected optical quality of the final beam, the crystallographic quality of the monochromators and of the beam expander is fundamental: the presence of crystallographic defects and of lattice plane curvature can broaden the X-ray reflectivity profiles of the crystals. In the BEaTriX error budget tree, 0.5 arcseconds HEW have been allocated for deviation from ideality of the crystals. A simple calculation shows that to maintain the horizontal divergence lower than 0.5 arcseconds along the 170 mm dimension of the expander crystal, the minimum acceptable curvature radius R of the reflecting planes is around 30 km.

As for the 4.51 keV beam line (TiKα line), the monochromators and the beam expander have been realized using extremely low doped, dislocation free silicon crystals characterized by a very high perfection. The very low doping prevents from the formation of residual strains in the material generated by non-uniform doping of the crystal during the crystal growth (Celotti *et al.*, 1974) and in the possible lattice bending.

The lower energy 1.49 keV beam line (AlKα line), corresponding to a wavelength of 8.314 Å, is more challenging as crystals with large lattice spacing are needed, involving materials less known than the widespread used silicon. For this wavelength range, the orthorhombic Ammonium Dihydrogen Phosphate (ADP) crystal is used for X-ray spectroscopy (Saint Gobain: https://www.crystals.saint-gobain.com/document/X-ray-monochromators): the lattice spacing (a=b=7.53 Å, c=7.742 Å) and structure permits to produce an intense (101) diffracted beam at θ_{Bragg}=51.417° for the AlKα wavelength.

ADP crystals are usually grown in large dimension by aqueous solution. They have been proposed more than 30 year ago for non linear optic applications (Moritani *et al.,* 1983). Their

structural characterization, performed by X-ray topography, confirmed that crystals are characterized by an elevated crystal perfection (Deslattes *et al*., 1966; Bhagavannarayan *et al*., 2006; Bhat *et al.*, 1983), nearly dislocation free and free of inclusions.

In order to assess if the commercially available ADP crystals can provide a crystal perfection compatible with the compelling requirements of the BEaTriX project, a detailed characterization is needed to check if they are free of dislocations and of other structural defects, and if the lattice planes are as flat as required, without bending due to the presence of residual strains.

2. Experimental

A 20×20×2 mm^3 ADP crystal, (001) oriented, was procured from Saint Gobain to perform preliminary analysis on its crystallographic quality. ADP crystal has an orthorhombic cell with a=b=7.53 Å e c=7.5420 Å and it is used for X-ray spectroscopy in the range of soft X-rays.

3. X-ray topography measurements

The X-ray topographic characterization has been performed by using a double crystal topographic camera using a copper anode ($\lambda_{CuK\alpha}$=1.54051 Å) and an asymmetrically cut Ge 620 perfect crystal as a monochromator with a Bragg angle of θ_B=59.6° (Jenichen *et al.*, 1988), not far from the (008) CuKα Bragg angle θ_B=54.79° of ADP, thus reducing the effect of wavelength dispersion due to the difference between Bragg angles of Ge monochromator and sample.

In the double crystal topographic camera, the wide beam impinges on the sample and the topograph is obtained by registering the diffracted beam on a film, while maintaining fixed the angle of incidence. The image reported in fig. 1a shows only the presence of a few surface scratches and of some isolated point defects, presumably emerging dislocations or tiny inclusions.

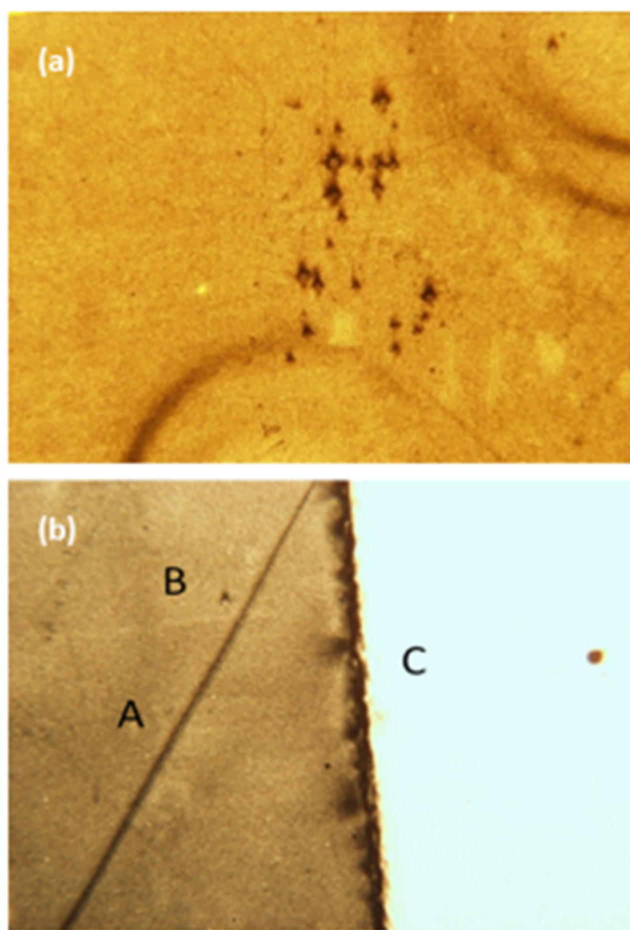

Figure 1 Double crystal topographs of the ADP sample. Ge 620 monochromator, CuKα_1 radiation. (a) 3x4 mm^2 area showing emerging dislocations or inclusions. (b) 3x4 mm^2 area near the edge of the crystal showing a scratch A, an emerging dislocation B and the contrast near the edge of the crystal C.

In Fig. 1b the x-ray topograph shows very few crystallographic defects, demonstrating the very high quality of the ADP crystal. The visible contrast near the edge of the crystal is clearly introduced by the cutting process. It is evident that the residual strain associated with the cutting process has not been removed by the etching or the polishing process and produces a characteristic strain contrast.

4. X-ray diffraction profile measurements

The measurements of X-ray diffraction profile and the full width at half maximum (FWHM) is considered a preliminary and effective test of the quality of the crystal, since the presence of defects always broadens the reflectivity profile. The theoretical diffraction profile, that corresponds to the perfect and strain free crystal, is calculated by using the dynamical theory of X-ray diffraction. The

calculation of the theoretical diffraction profile was obtained from Stepanov X-ray server (http://x-server.gmca.aps.anl.gov/) of Argonne National Laboratory after including in the database the ADP crystal structure. The (004) theoretical diffraction profiles for the σ polarization (electrical field perpendicular to the scattering plane) and for the π polarization for the CuKα radiation are reported in fig 2. The FWHM of σ and π profiles are 0.56 and 0.34 arcseconds respectively.

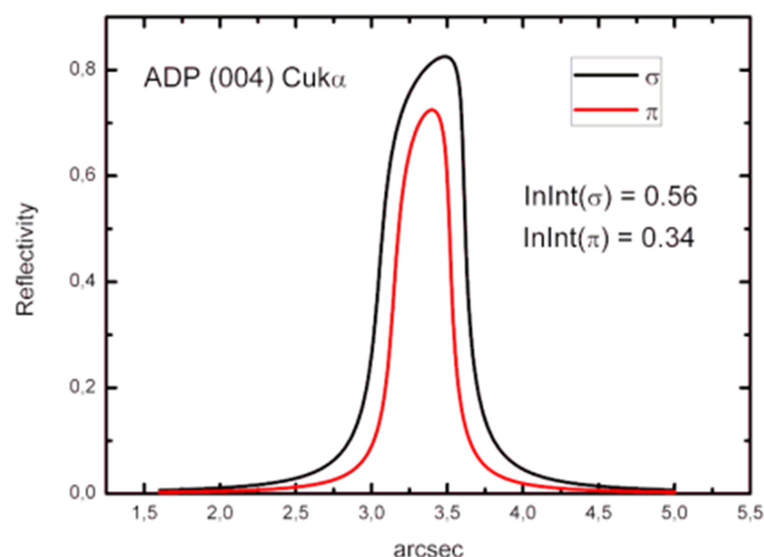

Figure 2 σ and π intrinsic diffraction profiles of ADP (004) at E=8.04 keV energy of X-ray beam as calculated by the Stepanov X-ray server (http://x server.gmca.aps.anl.gov/) of Argonne National Laboratory.

From the simulations it is clear that a direct measurement of the reflectivity profile is very difficult due to the need of a very parallel and monochromatic X-ray beam as a probe. An alternative method to verify the crystallographic quality of the sample is based on the measurement of the integrated intensity that is the area of the reflectivity profile normalized by the incident beam intensity, a parameter almost independent by the divergence and wavelength purity of the X-ray source.

The integrated intensity is a parameter very sensitive to the crystal quality. It has a minimum value for a perfect crystal and increases rapidly up to two order of magnitudes for ideally imperfect crystals (ideal mosaic) (Authier *et al.,*1998). The measurement has been performed in a Panalytical X-pert diffractometer using a 4 crystal Ge 220 monochromator, with a Ge 220 Bragg angle of θ_B=22.64°, not far from the (004) CuKα Bragg angle θ_B=24.112° of ADP, thus reducing the effect of wavelength dispersion.

For an accurate measurement it is necessary to take into account the polarization of the X-ray beam produced by the monochromator which is affected by the 4 Ge 220 reflections. The polarization

of the X-ray beam produced by the monochromator has been calculated by considering the σ and π profile of each Ge 220 reflection. Due to the 4 successive reflections the final profile of each component is calculated by taking 4th power of the intrinsic σ an π profiles. The resulting profiles have integrated intensities of 8.246 and 4.837 arcseconds respectively. It turns out that the exit beam is 63% σ and 37% π polarized respectively. In this way the expected integrated intensity of the ADP 004 reflection profile is

$$\mathrm{IntInt}_{\mathrm{theor}} = \frac{8.246}{8.246+4.837}\cdot 0.56 + \frac{4.837}{8.246+4.837}\cdot 0.34 = 0.48\ \mathrm{arcsec}$$

The ADP 004 experimental diffraction profile, normalized with the value of incident beam intensity is reported in fig. 4. As expected the experimental FWHM is much larger than the value predicted by simulation, but the value of the integrated intensity is close (~9% lower) to the value of perfect crystals. Since any structural defect or residual strain leads to an increase the integrated intensity, this demonstrates the excellent crystallographic quality of the sample and that the experimental FWHM is affected by the incident beam collimation and wavelength dispersion. A possible explanation of the lower experimental integrated intensity with respect to the simulated is the lack of Debye Waller attenuation factor in the ADP database used for the calculation.

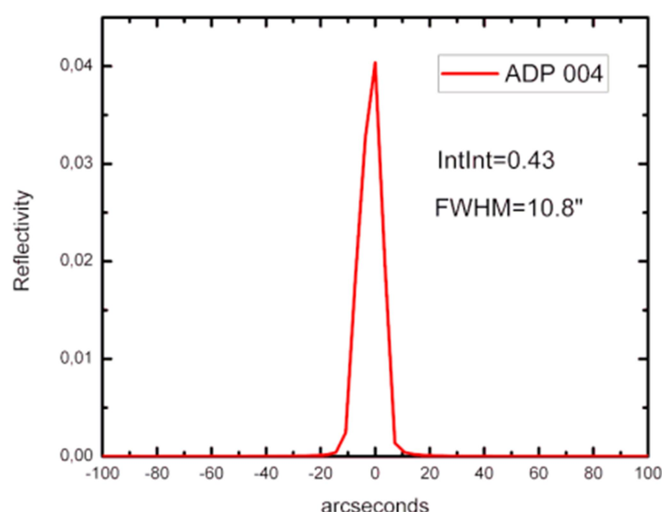

Figure 3 Experimental ADP (004) CuKα diffraction profile measured at Philips MRD diffractometer with a Bartels 4xGe220 monochromator.

5. Curvature Measurement

The second important parameter affecting the performances of the monochromator is the presence of a curvature in the crystal. From the allocated error of 0.5 arcseconds, a crystal of 120 mm length must have a minimum acceptable curvature radius of the order R=25 km. The curvature of the sample has been obtained by measuring the shift of the Bragg condition as a function of the position of the X-ray beam on the sample is applied (fig. 4). The Bragg condition shift $\delta\theta$ is related to the curvature R by $R=x/\delta\theta$, x being the distance between the two points of the measurement (Buffagni *et al.*, 2012). A linear dependence of the peak position shift as a function of position is an indication of a uniform curvature. In the geometry of our diffractometer a peak position shifting at higher angles at increasing x is an indication of a concave curvature.

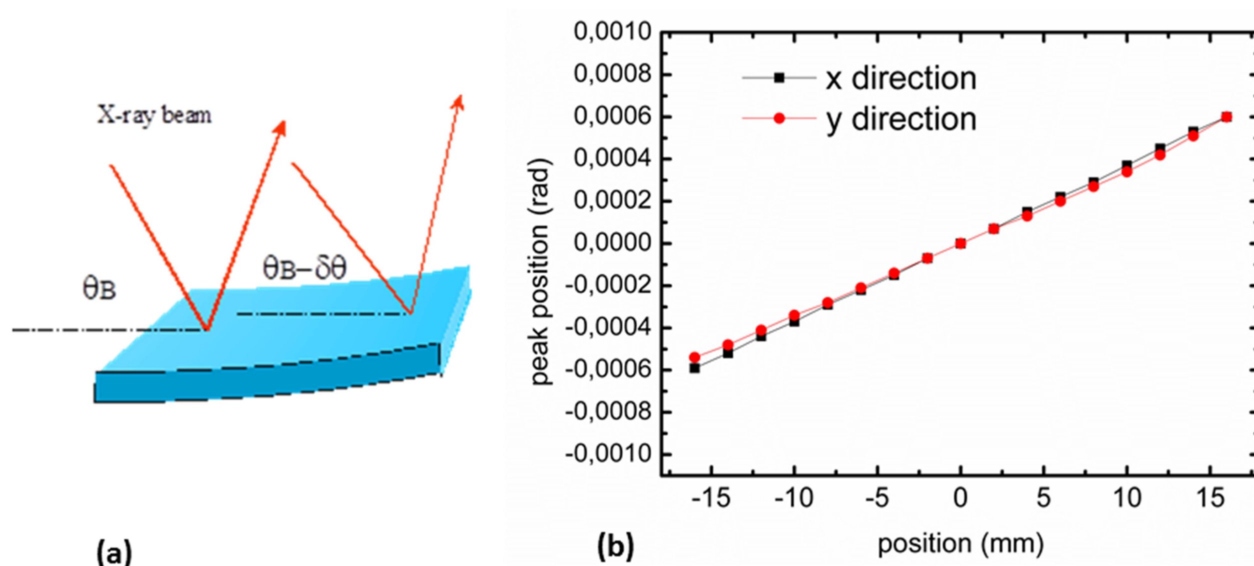

Figure 4 (a) Method of curvature measurement in large crystals. (b) Measurement of curvature in a spherically bent crystal with radius of curvature R=27 m.

To perform this measurement with the required accuracy, the translation stage of the crystal holder must be very reliable: for this purpose the stage of the diffractometer (Philips MRD) is based on the translation of the sample holder on a rectified surface. The system has been tested on a perfect silicon 2 mm thick sample. CuKα 004 reflectivity profiles taken with 5 mm spacing on the front and rear surface of a flat silicon wafer are reported in fig. 5.

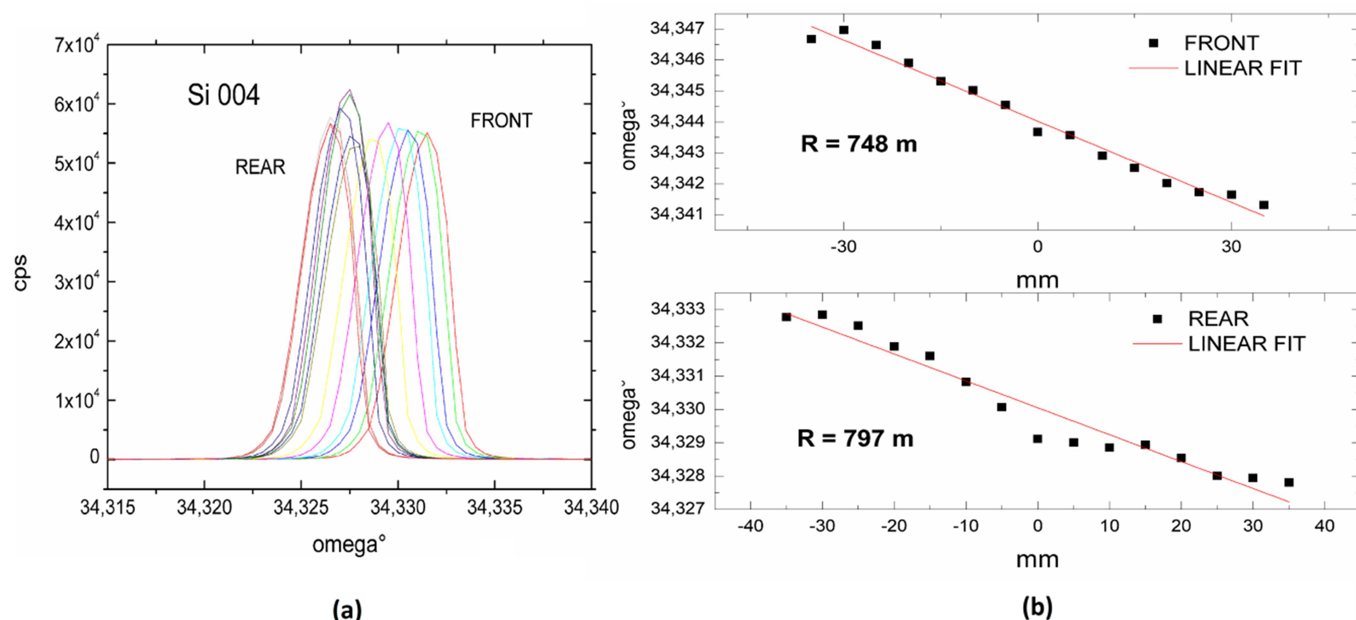

Figure 5 (a) 004 reflectivity profiles taken on both sides of the wafer with 5 mm spacing between adjacent points in a 70 mm range in a 2 mm thick perfect silicon crystal. (b) Bragg angle shifts measured on the front and rear surface. The apparent radius of curvature is reported.

The peak positions shifts, measured on both sides of the silicon wafer, are reported in fig. 5b. In both cases the Bragg peak positions decrease at x increasing. This demonstrates that the calculated curvature is apparent, and that the shifts are due to the mechanical inaccuracy of the translation stage. By repeating the measurements on the same side nearly identical results are obtained.

Similar measurements have been performed on the $20\times20\times2$ mm^3 ADP sample using the ADP (004) reflection. The experimental curves are reported in fig 6a and the shift of the Bragg condition as a function of the position in fig 6b. The peak position shift reported in fig. 6b are compensated by the mechanical inaccuracy of the translation stage. In this way a R=1350 m concave curvature is obtained, a value much smaller than the required value of 25 km.

The most reasonable explanation of the curvature is the presence of residual strain associated to the not polished side of the sample. It is in fact well known that the surface damage introduces a local compressive strain and produces a convex curvature of the sample on the damaged side (Ferrari *et al.*, 2013), and concave at the opposite side, as in the present case. This hypothesis is confirmed by the presence of strain at the edges of the crystal, as observed in the topograph of fig. 1b. New measurements on a double side ADP sample are planned, to fully validate this hypothesis.

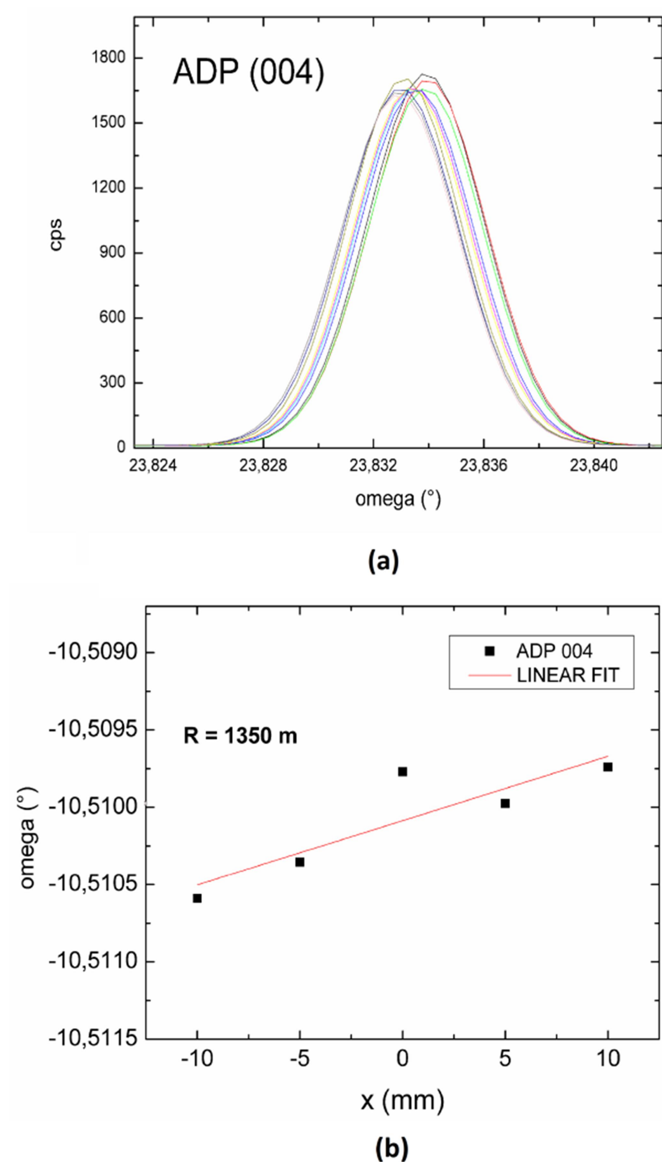

Figure 6 (a) ADP 004 reflectivity profiles spaced 2 mm between adjacent points in a 20 mm range. (b) Bragg angle condition shift in a 20 mm range of the ADP 004 reflectivity profiles.

For the application in the BEaTriX facility, a beam expander crystal thicker than 2 mm (the thickness of the present sample) will be considered in order to increase the rigidity of the piece. In case of a resulting beam expander with curvature above specifications, possible recovery actions will include the use of a bending system to compensate for the residual curvature.

6. Conclusion

ADP organic crystals have been considered to realize the monochromator and beam expander of the 1.49 keV beam line of the BEaTriX facility, meant to test the Silicon Pore Optics modules of the

ATHENA X-ray telescope. For this application it is of fundamental importance that the crystals are free of structural defects, such as dislocations and inclusions, and the lattice planes are perfectly flat. To assess the possible use of ADP for this application, we have characterized a 20×20×2 mm^3 ADP commercial sample by X-ray topography and reflectivity profile measurements.

As for the point of view of the crystallographic quality, a X-ray topograph showed very few dislocations, and surface scratches, almost compatible with the proposed application. Moreover accurate measurements of the integrated intensity of the CuKα(004) reflectivity profile gave results in line with that expected for a perfect crystal.

The lattice curvature measured with the method of Bragg condition variation as a function of the position showed a curvature of the sample R=1350 m, much smaller than the acceptable bending radius of lattice planes for the BEaTriX facility. Further tests on double side polished ADP sample are planned to check if the curvature is due to the residual stress of the second unpolished side in the present sample. A final recovery action is anyway defined, and foresees the application of an elastic bending to the crystal to compensate the spontaneous curvature.

Acknowledgements The study of BEaTriX started in 2012 supported by a AHEAD H2020 project and also supported by an ESA contract. Authors are grateful to dr. Ivo Ferreira and dr. Marcos Bavdaz for ESA referring and support.

References

Authier, A., Malgrange, C. (1998). *Acta Cryst.* **A54**, 806-819.
Bhat, H. L., Roberts, K. J., Sherwood, J. N. (1983). *J. Appl. Cryst.* **16**, 390-398.
Bhagavannarayana, G., Parthibanb, S., Meenakshisundaram, S. (2006). *J. Appl. Cryst.* **39**, 784–790.
Buffagni, E., Ferrari, C., Rossi, F., Marchini, L., Zappettini, A. (2012). *Optical Engineering* **51(5)**, 056501.
Celotti, G., Nobili, D., Ostoja, P. (1974). *J. Mater. Sci.* **9(5)**, 821-828.
Deslattes, R. D., Torgesen, J. L., Paretzkin, B., Horton, A. T. (1966). *J. Appl. Phys*. **37,** 541.
Ferrari, C., Buffagni, E., Bonnini, E., Korytar, D. (2013). *J. Appl. Cryst.* **46(6)**, 1576-1581.
Jenichen, B., Kohler, R., Mohling, W. (1988). *J. Phys. E: Sci. Instrum.* ***21,*** 1062-1066.
Moritani, A., Okuda, Y., Nakai, J. (1983). *Appl. Opt.* **22(9)**, 1329-1336.
Pelliciari, C., Spiga, D., Bonnini, E., et al., (2015). *Proc. SPIE* **9603**, 96031P.
Salmaso, B., Spiga, D., Basso, S., et al. (2018). *Proc. SPIE* **10699***,* 106993I.
Sanchez del Rio, M., Cerrina, F. (1992). *Rev. Sci. Instrum.* **63**, 936.

Spiga, D., Pelliciari, C., Bonnini, E., et al. (2014). *Proc. SPIE* **9144**, 91445I.

Spiga, D., Pareschi, G., Pelliciari, C., et al. (2012). *Proc. SPIE* **8443**, 84435F.

Spiga, D., Pelliciari, C., Salmaso, B., et al. (2016). *Proc. SPIE* **9963**, 996304.